

# Biogenic Functionalized ZnO/CuO Nanocomposite Sensor for Potentiometric Determination of Pseudoephedrine-HCl in Pure and Commercial Products

Fadam M. Abdoon\*<sup>1</sup>  , Sarhan A. Salman<sup>1</sup>  , Hasan M. Hasan<sup>2</sup>  , Suham T. Ameen<sup>3</sup>  , Maha F. El-Tohamy<sup>4</sup>  

<sup>1</sup>Department of Chemistry, College of Science, Tikrit University, Tikrit, Iraq.

<sup>2</sup>College of Pharmacy, Tikrit University, Tikrit, Iraq.

<sup>3</sup>College of Health and Medical Technology, Uruk University, Baghdad, Iraq.

<sup>4</sup>Department of Chemistry, College of Science, King Saud University, P.O. Box 22452, Riyadh 11495, Saudi Arabia.

\*Corresponding author.

Received 09/09/2023, Revised 22/10/2023, Accepted 24/10/2023, Published Online First 20/03/2024,  
Published 01/10/2024



© 2022 The Author(s). Published by College of Science for Women, University of Baghdad.

This is an open-access article distributed under the terms of the [Creative Commons Attribution 4.0 International License](https://creativecommons.org/licenses/by/4.0/), which permits unrestricted use, distribution, and reproduction in any medium, provided the original work is properly cited.

## Abstract

The ultrafunctional potential of zinc oxide (ZnO) and copper oxide (CuO) nanoparticles (NPs) has generated a great interest in using such metal oxides as remarkable and electroactive nanocomposites in the studies on potentiometry and sensors. These nano-oxides were prepared from the extract of *Leucaena leucocephala* seeds as an environmentally friendly process. The development of a ZnO/CuO “core-shell modified-nanocomposite” coated copper wire film sensor was proposed as a new method for potentiometric determination of pseudoephedrine hydrochloride (PSD) in pure and pharmaceutical dosage forms. With the existence of polyvinyl chloride (PVC) as a polymer with high molecular weight and “*o*-nitrophenyl octyl ether (*o*-NPOE) as a solvent mediator”, PSD was combined with phosphotungstic acid (PTA) to produce pseudoephedrine hydrochloride-phosphotungstate (PSD-PT) as a sensing substance. The improved sensor showed a very high sensitivity and selectivity for determining and quantifying the PSD with a linear relationship of  $1.0 \times 10^{-8}$ – $1.0 \times 10^{-2}$  mol L<sup>-1</sup>. It was estimated that the regression equation was represented by the  $EmV = (-58.143) \log [PSD] + 526.71$ . With the proposed sensors, pseudoephedrine hydrochloride could be effectively determined in pure and commercial product forms.

**Keywords:** Green Chemistry, *Leucaena leucocephala*, Polymeric Sensor, Pseudoephedrine HCl, ZnO/CuO nanocomposite.

## Introduction

In recent years, green chemistry has played a significant role in analytical chemistry, especially by using fruits, leaves, and seeds of plants available in public, private gardens, or in nature<sup>1</sup>. The methods for synthesizing nanomaterials from these plant sources have evolved to produce hybrid nanomaterials instead of single nanoparticles<sup>2</sup>. Several articles have been published to investigate

the exceptional properties of metal oxides such as ZnO, Al<sub>2</sub>O<sub>3</sub>, CuO, and MgO, etc. The use of zinc oxide and copper oxide nanoparticles (ZnONPs and CuONPs) with large surface areas and unique properties such as specific catalytic, optical, chemical, and mechanical properties have attracted much attention<sup>3-6</sup>. In addition to coating the sensor wire to improve the catalytic properties of the

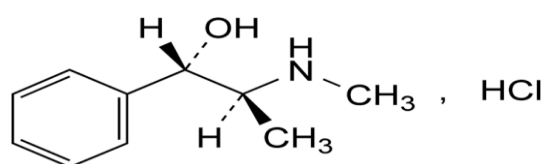
substrate, the development of a nanocomposite of metal oxide ensures the interaction between the base metal materials and the base medium<sup>7-10</sup>.

The ZnO/CuO nanocomposite is also widely used in catalysis. The application of this nanocomposite in electrochemical sensors is promoted by the multifunctional physicochemical potential of ZnONPs and CuONPs as well as their large surface area, strong binding properties, and good isoelectric stability<sup>11-14</sup>.

*Leucaena leucocephala* is a tiny, fast-growing tree that has spread across the tropics and into portions of Asia<sup>15</sup>. This plant is a fast-growing medium-sized tree of the Fabaceae family. Therapeutic properties of *Leucaena leucocephala* include relieving stomach discomfort, contraception, and abortion. Sulfated glycosylated polysaccharides extracted from the seeds have been shown to have significant anticancer chemo preventive and antiproliferative effects<sup>16</sup>.

In tablet formulations, the seed gum is used as a binder<sup>17</sup>. *Leucaena leucocephala* plant extract has potential antidiabetic, antimicrobial, and anthelmintic effects<sup>18</sup>. The dyes obtained from this plant can also be used in the leather and cotton industries<sup>19,20</sup>. Accordingly, in the current work, the seed extract of *Leucaena leucocephala*, a medicinally important plant, was used for the green synthesis of the ZnO/CuO nanocomposite. The seed extract is used as a reducing and stabilizing agent.

Pseudoephedrine hydrochloride (PSD) is a decongestant that causes constriction of the blood vessels in the nasal passages. Nasal congestion may be caused by dilated blood vessels. Pseudoephedrine is used to relieve nasal and sinus congestion and congestion of the eustachian tubes, which drain fluid from the inner ears. It is a sympathomimetic from the phenethylamine and amphetamine chemical family<sup>21</sup>. Chemically, PSD is identified as (1S,2S)-2-(methylamino)-1-phenylpropan-1-ol hydrochloride Fig 1. It is a white crystalline powder or colorless crystals that are slightly soluble in water and ethanol (96%) and sparingly soluble in methylene chloride. Its melting point is about 184 °C<sup>22</sup>.



## Materials and Methods

### Figure 1. Chemical structure of pseudoephedrine HCl (mwt: 201.69 g/mol, molecular formula: C<sub>10</sub>H<sub>16</sub>NOCl)

In the past, numerous analytical methods, such as spectrophotometric methods<sup>23,24</sup>, have been used to determine PSD. Separation methods such as liquid chromatography<sup>25,26</sup>, liquid chromatography-tandem mass spectrometry<sup>27</sup>, capillary zone electrophoresis<sup>28</sup>, and voltammetric method<sup>29</sup> have also been described and developed for the determination of PSD.

Electrochemical methods, such as conductometry, potentiometry, and amperometry are more reliable and cost-effective for chemical detection, chemical and biosensing applications<sup>30-33</sup>. These approaches are also fast in terms of analysis time, allowing on-line detection of aqueous solutions. The potentiometric approach is one of the most efficient self-powered techniques, with potential difference determination produced by the electrostatic buildup of analytes on the surface of the working sensor and the reference sensor. Several potentiometric sensors have recently been functionalized with metal oxides nanoparticles or nanocomposites to improve their sensitivity and detection limits<sup>34-36</sup>. However, only one potentiometric sensing method based on nano-metal oxides was reported for the determination of PSD<sup>30</sup>, and no method was proposed for the quantification of PSD in a strategy modified with core-shell nanocomposites (metal oxide/metal oxide NP). The previously mentioned techniques showed good sensitivity for the quantification of PSD. However, they have certain limitations due to the long analysis times, the great experience of analysts, and the use of solvents. The aim of the suggested approach is to produce a modified PSD-PT-ZnO/CuO nanocomposite sensor that is both extremely sensitive and selective. This manufactured sensor was designed for potentiometrically measuring the pharmaceutical and pure forms of sympathomimetic PSD. The method used in this study was validated to certify the appropriateness of the amended coated sensors.

## Instruments

A pH/mV (JENWAY 3310 UK) and a pH/mV (pH700, EUTECH Instruments, Singapore) were used for the potentiometric measurement. The nanocomposites' UV-vis spectra were measured using a Shimadzu-1800 spectrophotometer (Shimadzu Ltd, Tokyo, Japan). In order to determine the dimensions and shape of the metal nanocomposites, a scanning electron microscope (Mira3, SEM) (Czech Republic) was used at 15kV and x10 magnification. To capture the X-ray powder diffractogram (XRD), we employed a D-5000 diffractometer from Siemens (Germany). The Fourier transform infrared (FTIR) spectra were analyzed using a Shimadzu FT-IR 8400S spectrophotometer (Tokyo, Japan).

## Chemicals

Samarra Drug Industry (SDI), an Iraqi company, provided the pure grade of PSD. One, Two, Three (1,2,3)® syrup (Hikma Pharma S. A. E., Egypt) 15mg/5mL, Acetamol® tablet (Sama Alfayhaa Pharmaceutical company, Basra, Iraq) 30mg/ Tablet and Congestal® (SIGMA Pharmaceutical Industries, Quesna, Egypt) 60mg/tablet were purchased from a nearby local pharmacy. Various chemicals and solvents, including THF 99.0%, PTA 99.9%, acetone 99.8%, *o*-NPOE, HCl 37% and polyvinyl chloride (PVC) of a high molecular weight were purchased from Sigma Aldrich (Hamburg, Germany). BDH (Poole, UK) supplied the zinc nitrate hexahydrate, copper nitrate trihydrate, and NaOH. A robustness study used phosphate buffer 5.5 (Merk, Darmstadt, Germany) to adjust pH. Analytical-grade reagents were used throughout.

## Green Synthesis of ZnO/CuO Nanocomposite Collection and Preparation of *Leucaena leucocephala* Seeds

*Leucaena leucocephala* seeds samples were collected freshly from Tikrit University Gardens (Tikrit, Iraq) in February 2023. Deionized water was used to wash the seeds to be used after drying at 60 °C for 28 hrs. Five grams of seeds were well crushed and added to 150 mL of deionized water with stirring at 60 °C for 4 hrs. The extract was separated by centrifugation (at least 10 minutes and 6000 rpm) to remove suspended solids. The extract was collected for the preparation of ZnONPs<sup>37,38</sup>.

## Green Synthesis ZnO/CuO Nanocomposite

For the formation of the ZnO-CuO nanocomposite, 0.72 g of zinc nitrate and 0.19 g of copper nitrate were mixed into 80 mL of deionized water to produce concentrations of 0.03 mol L<sup>-1</sup> Zn(NO<sub>3</sub>)<sub>2</sub> and 0.01 mol L<sup>-1</sup> Cu(NO<sub>3</sub>)<sub>2</sub>. To create a mixed colloid of these metals hydroxides (Zn(OH)<sub>2</sub>) and Cu(OH)<sub>2</sub>, 20 mL of seed extract was added to the previous solution while stirring at laboratory temperature, and the pH was adjusted to 10. The ultracentrifuge was used to separate the colloid and then dry it. The colloid was then calcinated for 4 hours at 400 °C. The phytochemicals present in seed extract such as saponins, flavonoids, phenols, cardiac glycosides, and tannins, phlobatannin and terpenoids as secondary metabolites such as strong reducing and stabilizing agents during the green synthesis of nanoparticles process<sup>39</sup>. The formation of ZnO/CuO nanocomposites was demonstrated by observing the blue color of the powder<sup>40,41</sup>. The steps of synthesizing the nanocomposite of ZnO-CuO are shown in Scheme 1.



**Scheme 1. Schematic steps for the green synthesis of ZnO/CuO nanocomposites**

### Characterization of ZnO/CuO Nanocomposite

Spectroscopic measurements were carried out at 200–600 nm wavelength to ensure the ZnO/CuO nanocomposite creation. In addition, FT-IR was performed to define the potential practical sets that may exist in the synthesized ZnO/CuO nanocomposite. XRD analysis thoroughly used “K $\alpha$  radiation ( $\lambda = 1.5418 \text{ \AA}$ ) under an operative current of 35 mA”. SEM was used to specify the morphology of surface, size distribution and shape.

### Preparing the PSD Stock Solution and Pharmaceutical Dosage Forms

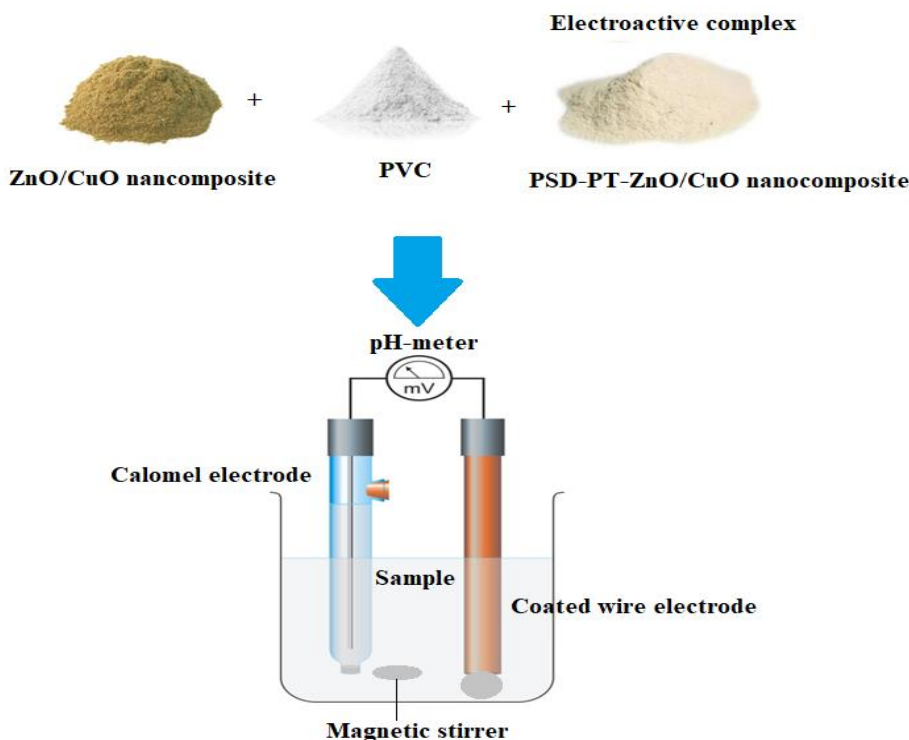
Here, 0.2017 g of PSD was dissolved in 100 mL of deionized water to obtain a standard solution of  $1.0 \times 10^{-2} \text{ mol L}^{-1}$  PSD. The following commercial dosage formulations were prepared: 1, 2, 3 $\text{\textcircled{R}}$  syrup solution was diluted 67.2 mL in a 100 mL volumetric flask to obtain a  $1.0 \times 10^{-2} \text{ mol L}^{-1}$  of the pure PSD solution. Ten Acetamol $\text{\textcircled{R}}$  tablets weighed 2.103 g. Then, 1.414 g was dissolved in a 100 mL volumetric flask to prepare the pure PSD's final solution of  $1.0 \times 10^{-2} \text{ mol L}^{-1}$ . 1.2354 g of the pure PSD from Congestal $\text{\textcircled{R}}$  tablets was also obtained by dissolving 1.2354 g from a combination of ten tablets (the weight of ten tablets was 3.675 g). A series of dilutions prepared all lower concentrations.

### Preparing the Electroactive Ion-pair

In this step, 50 mL of an aqueous PSD solution was added to the same volume of PTA solution at the same concentration of  $1.0 \times 10^{-2} \text{ mol L}^{-1}$  to obtain the electroactive ion-pair of PSD-PT. Then, deionized water was used to form, filter and thoroughly wash a white precipitate of PSD-PM. After that, this white precipitate was left to dry at room temperature for at least two days.

### Fabrication of Sensor and Membrane Compositions

The combination of 5 mg of the formerly manufactured nanocomposite of ZnO/CuO, 10 mg PSD-PT, 190 mg PVC, 0.35 mL *o*-NPOE as a plasticizer, and 5 mL THF was used to prepare the PSD-PT-ZnO/CuO sensor. The sensor was fabricated by continuously dipping washed copper wire into the membrane solution until the coated area had been obtained. This was done after the wire tip was cleaned and dried using distilled water and acetone<sup>30</sup>. The coated wire sensor was constructed using: copper wire/fabricated sensor/investigated drug solution/Hg/Hg<sub>2</sub>Cl<sub>2</sub> (reference electrode). Scheme 2 shows the fabrication of the polymer-coated wire membrane cocktail and the setup of the potentiometric system.



**Scheme 2.** The scheme of creating the potentiometric system and PSD-PT-ZnO/CuO nanocomposite sensor.

### Calibration Curve

The calibration curve of the PSD-PT-ZnO/CuO nanocomposite sensor was prepared by recording the potential responses of 25 mL PSD standard solution over the concentration range of  $1.0 \times 10^{-8}$ - $1.0 \times 10^{-2}$  mol L<sup>-1</sup> using the constructed sensor separately in conjunction with a calomel reference electrode (Hg/Hg<sub>2</sub>Cl<sub>2</sub>). The plot of calibration for the above sensor was made by plotting the potential values as a function of -log PSD concentrations. The distilled water was used to thoroughly clean the surface of sensors, and then tissue paper was used to dry this surface before each measurement.

### The Optimal Conditions

The suggested sensor's potential measurements are highly sensitive to changes in pH. To assess the optimal pH range for the constructed sensor,  $1.0 \times 10^{-2}$  and  $1.0 \times 10^{-4}$  mol L<sup>-1</sup> PSD test solutions were acidified with 0.1 mol L<sup>-1</sup> hydrochloric acid to decrease the pH and 0.1 mol L<sup>-1</sup> sodium hydroxide to increase the pH. The optimum pH diagram was

drawn by plotting the suggested sensor potential against the values of pH.

A separate solution method (SSM) was used to test the PSD-PT-ZnO/CuO nanocomposite sensor selectivity<sup>42</sup>.

The sensor's potentiometric selectivity coefficient was estimated by preparing separate solutions of each  $1.0 \times 10^{-3}$  mol L<sup>-1</sup> PSD and some interfering species, such as 1<sup>st</sup>, 2<sup>nd</sup>, and 3<sup>rd</sup> cations and anions, sugars, amino acids, and polysaccharides. The equation of SSM was used to calculate the selectivity coefficient as follows:

$$\text{“Log Kpot} = (E_2 - E_1)/S + \text{Log [PSD]} - \text{Log [B}^{z+}]^{1/z}\text{”}$$

Where “Kpot” is the coefficient of selectivity, “E<sub>1</sub>” and E<sub>2</sub>” are the electrode potential of  $1.0 \times 10^{-3}$  mol L<sup>-1</sup> of PSD solution while B<sup>z+</sup> and S are the electrode potential of  $1.0 \times 10^{-3}$  mol L<sup>-1</sup> of interfering species and slope of the calibration curve, respectively.

The dynamic response time was investigated by calculating the tested drug's potential response using the concentration range of  $1.0 \times 10^{-8}$ - $1.0 \times 10^{-2}$  mol L<sup>-1</sup>.

## Results and Discussion

### Characterization of the ZnO/CuO Nanocomposite

The preparation of ZnO/CuO nanocomposite has been characterized by various spectroscopic methods, including ultraviolet-visible, FT-IR, SEM and XRD. To verify the original identification of the size, shape, and stability of the synthesized nanoparticles of metal oxide in their aqueous suspensions, ultraviolet spectroscopy was revealed to be a useful technique. The UV-Vis spectra of the

ZnO/CuO nanocomposite presented the following absorption at 340 nm and 378 nm, Fig. 2. The following equation<sup>10</sup> was used to estimate the direct optical band gaps of the synthesized ZnONPs and CuONPs: **E<sub>g</sub> = hc/λ 1.**

E<sub>g</sub> is the energy, while h, C, and λ represent the “constant of Planck (6.62610<sup>-34</sup> J.s)”, the “light speed (2.99×10<sup>8</sup> m/sec)”, and the wavelength, respectively. Above ZnO and CuO NPs were predicted to have band gaps of 3.65 eV and 3.28 eV, respectively.

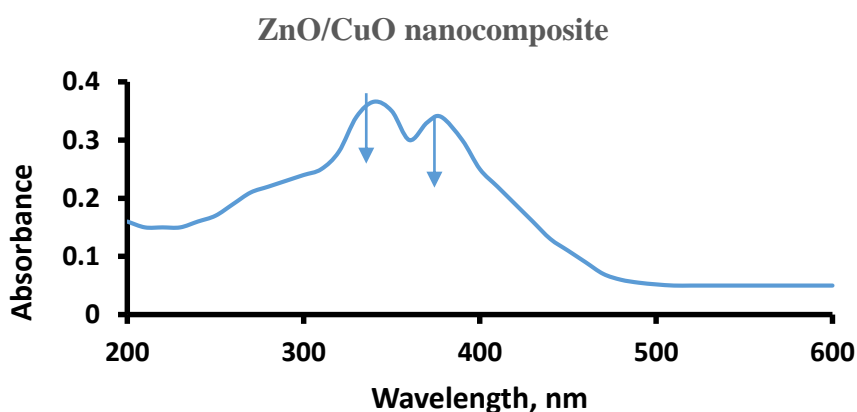
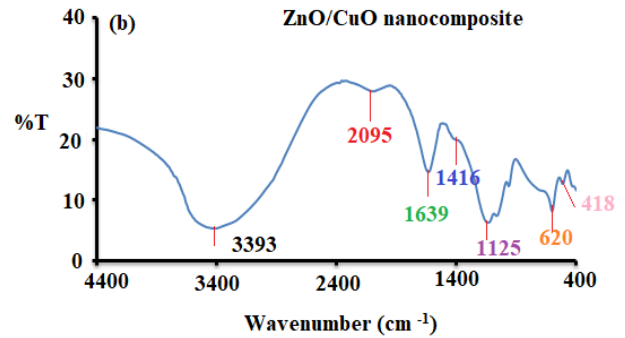
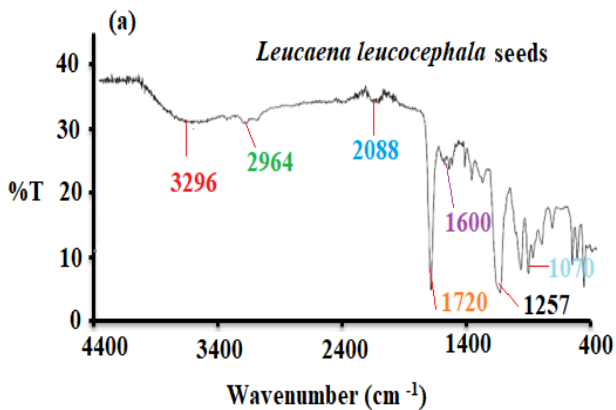


Figure 2. The spectrum of UV-Vis of the manufactured nanocomposite of ZnO/CuO (0.01% w/v) using deionized water.

In order to increase the probability of scattering and penetrating radiation, surface plasmon resonance (SPR) reduces the surface. These processes accelerate oxidation because they lead to the creation of surface holes and the separation of electrons. Variations in the dielectric matrix can also affect absorption peaks on an SPR. It is well-established that the matrix's refractive index directly affects its effective dielectric behavior.

FT-IR spectroscopy is also used to identify the functional groups contributing to ZnO/CuO nanocomposites synthesis. The FT-IR spectrum of *Leucaena leucocephala* seeds extract shows the presence of different absorption peaks at 3296, 2964, 2088, 1720, 1600, 1257, and 1070  $\text{cm}^{-1}$  due to the presence of (strong broad O-H of alcohol), (N=C=S stretching of isocyanate), (Strong C=O stretching of conjugated anhydride), (Strong C=O stretching of  $\delta$  lactam), (Strong C-O stretching of alkyl aryl ether), and (Strong S=O stretching of sulfoxide), respectively Fig. 3.



**Figure 3. FT-IR spectra of (a) *leucocephala* seeds extract and (b) synthesized ZnO/CuO nanocomposite using *Leucaena leucocephala* seeds extract at a wavenumber range from 4400 to 400  $\text{cm}^{-1}$ .**

The FT-IR spectrum of ZnO/CuO nanocomposite shows the presence of seven significant absorption peaks at 3393, 2095, 1639, 1416, 1125, 620, and 418  $\text{cm}^{-1}$  related to (Strong, broad O-H of phenolic compounds), (Strong N=C=S stretching of isothiocyanate), (Medium, C=C stretching of alkene), (Medium, O-H of alcohol), (Strong C-O stretching of tertiary alcohol), (Cu-O stretching), and (Zn-O stretching mode).

SEM was used at different magnifications to conduct additional microscopic research on the size, shape and morphology of surface of the produced ZnO-CuO NPs. The images of SEM showed the identical distribution of nanoparticles that have spherical and hexagonal shapes for ZnONPs and CuONPs, respectively. While the particle size of ZnO/CuO nanocomposite was in the range of 80 to 100 nm with highly accumulated crystals in their surface morphology Figs. 4a and 4b.

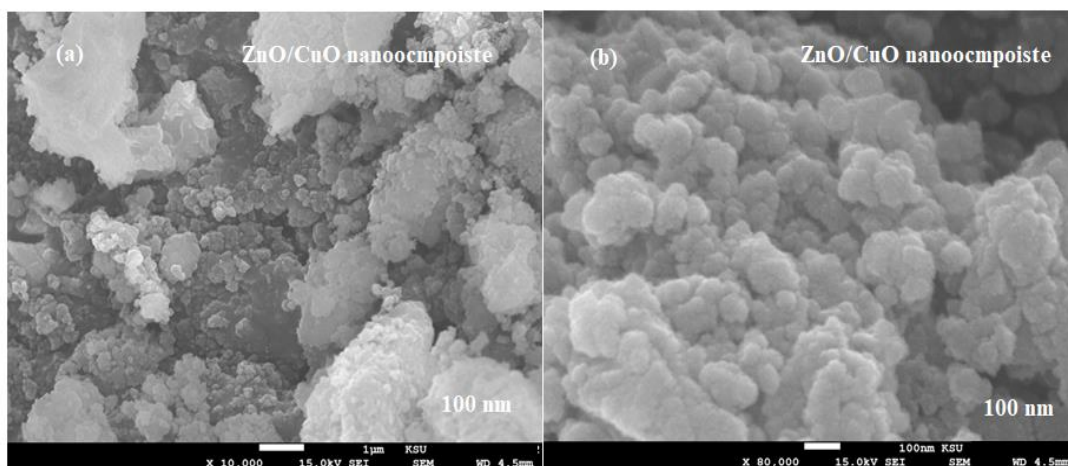


**Figure 4. a&b SEM micrographs of ZnO/CuO nanocomposite at 10,000 x and 80,000x magnifications.**

The X-ray diffraction patterns were discovered throughout a 20-100° 2θ range to analyse the crystal structure of green synthesized ZnONPs and CuONPs. Fig.5a shows clear and prominent peaks, indicating that the produced metal oxide nanoparticles have outstanding crystallinity with roughly bigger crystallites and takes into account the impact of synthesis conditions on crystal nucleation and growth. ZnONPs had substantial maxima at 31.64° (100), 34.43° (002), 36.29° (101), 47.75° (102), 56.51° (110), 62.90° (103), 67.98° (112), and 69.23° (112). The results matched the ZnO standard card No. 36-1451<sup>43,44</sup>.

The crystalline structure of green synthesized CuONPs was confirmed by the XRD analysis Fig.5b

Various diffraction peaks at 2θ of 32.61° (1 1 0), 35.64° (0 0 2), 38.97° (1 1 1), 48.93° (0 2 0), 53.55° (2 0 2), 58.35° (1 1 3), 61.08° (0 2 2), 66.27° (3 1 1), and 79.27° (2 2 2) showed the monoclinical spherical crystalline nature. The results matched the CuO standard card no. 48-1548<sup>45</sup>. Fig. 5c shows the presence of both ZnO and CuO peaks indicating the successful formation of ZnO/CuO nanocomposite.

The average crystalline size of ZnO/CuO nanocomposite was calculated using the Debye-Scherrer formula,  $D = 0.89\lambda / \beta \cos\theta$ . Where  $\lambda$  (1.54 Å) is the wavelength of the X-ray,  $\theta$  is Bragg's diffraction angle and  $\beta$  is the full width at half maximum. The estimated crystalline size was 17.64 nm.

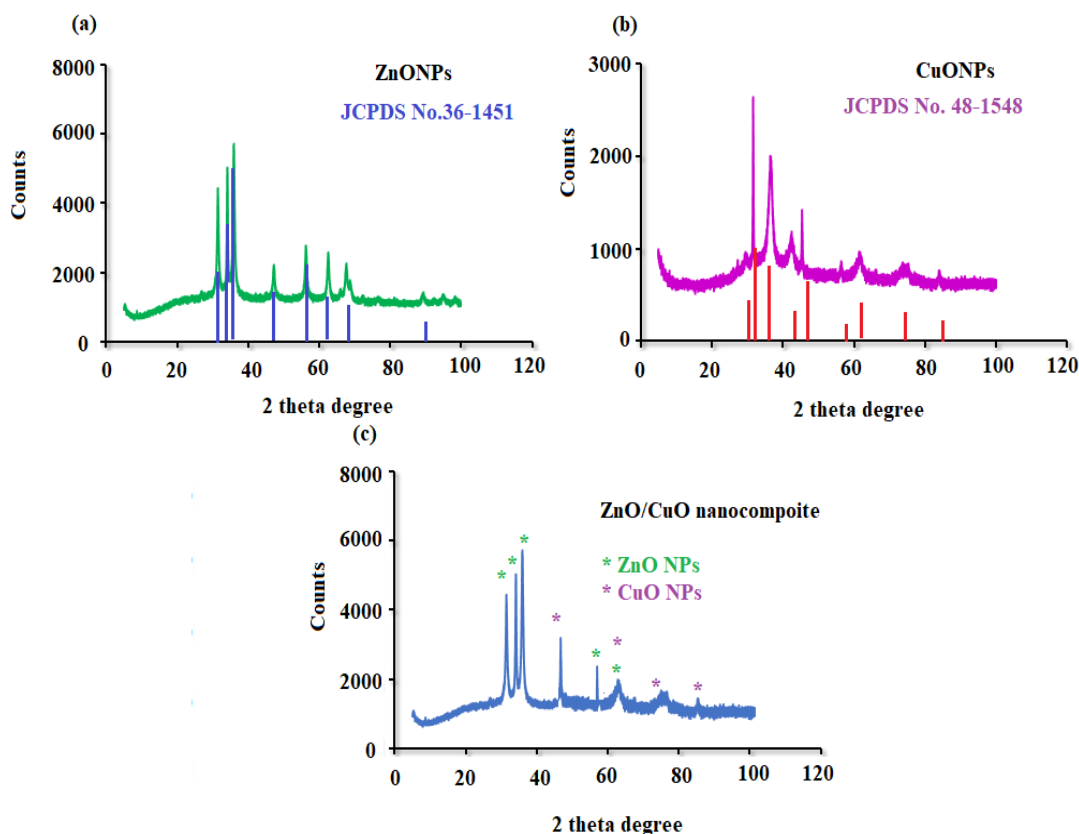


**Figure 5. The XRD spectra of (a) ZnONPs, (b) CuONPs, and (c) ZnO/CuO nanocomposite measured at 20-100° 2θ degree.**

### Optimization of Membrane Composition

In general, the features and qualities of a sensor, such as sensitivity, selectivity, a lifetime and other parameters, are affected by the amount and kind of plasticizer, polymer matrix, and solvent used<sup>46</sup>. In this study the effect of different membrane compositions on their characteristics were

investigated. Table.1 summarizes the optimization of membrane composition. The obtained results revealed that the excellent potential readings were observed by using the sensor 1 and 2 with slope -58.5 mV decade<sup>-1</sup>. Therefore, these percentages were used in further studies.

**Table 1. Effect of membrane composition on the potential readings of the modified PSD-PT-ZnO/CuO nanocomposite sensor**

No.	Plasticizer (%) <i>o</i> -NPOE	PVC (%)	Ion-pair (%)	THF (mL)	Slope (mV)
1	66	33	2	5	-58.5
2	66	33	2	5	-58.5
3	63	33	4	5	-56.3
4	63	33	4	5	-56.3
5	60	33	6	5	-53.7
6	60	33	6	5	-53.7

**The Nature of the Constructed Modified PSD-PT-ZnO/CuO Nanocomposite Sensor**

PSD reacts with PTA to produce the stable PSD-PM complex, which is soluble in organic solvents like THF. The PSD-PT-ZnO/CuO nanocomposite sensor was prepared by combining the above components in THF with a mediating solvent (*o*-NPOE) and polyvinyl chloride. In this study, *o*-NPOE acts as a plasticizer supporting the electroactive substance's homogeneous dissolution. The selectivity of the proposed PSD-PT-ZnO/CuO nanocomposite sensor towards the investigated PSD analyte has been enhanced using *o*-NPOE with a high dielectric constant ( $\epsilon = 24$ )<sup>47</sup>.

Table 2 summarizes the expected response and important performance characteristics of the proposed PSD-PT-ZnO/CuO nanocomposite. The

surface of the Cu wire sensor was coated with a sensing membrane combination, resulting in many electroactive spots on the sensor surface. Metal oxide nanoparticles with different physical and chemical properties, such as the ZnO/CuO nanocomposite, were incorporated into the membrane composition to enhance the conductivity of the sensor surface due to their mechanical and chemical stability, high dielectric constant, high conductivity, and large surface area, which increase the PSD ions in the sample solution and the active sites distributed on the membrane surface.

Results showed that the suggested sensor exhibited Nernstian response with the slope of  $E_{mV} = (-58.143) \log [\text{PSD}] + 526.71$  over the PSD concentration range of  $1.0 \times 10^{-8}$ - $1.0 \times 10^{-2} \text{ mol L}^{-1}$  with a correlation coefficient 0.9995 for PSD-PT-ZnO/CuO nanocomposite sensor Fig. 6.

**Table 2. The outcomes data for ZnO/CuO nanocomposite coated wire pseudoephedrine hydrochloride phosphotungstate sensor**

Parameter	PSD-PT-ZnO/CuO nanocomposite sensor
Equation of regression	$E_{mV} = (-58.143) \log [\text{PSD}] + 526.71$
Correlation coefficient, (r)	0.9995
Slope, (mV/decade) $\pm$ SD	58.143 $\pm$ 0.2
Intercept	526.71
Linearity, mol L <sup>-1</sup>	$1.0 \times 10^{-8}$ - $1.0 \times 10^{-2}$
Working pH range	3-6
Temperature, (°C)	25
LOD, (mol L <sup>-1</sup> )	$5.2 \times 10^{-9}$
LOQ (mol L <sup>-1</sup> )	$1.0 \times 10^{-8}$
Response time, (s)	30
Lifetime, (day)	80
Accuracy, (%) $\pm$ SD	99.6 $\pm$ 0.3
Robustness, (%) $\pm$ SD	98.3 $\pm$ 1.50
Ruggedness, (%) $\pm$ SD	99.1 $\pm$ 0.98

The sensing mechanism was summarized as follows: The surface of the copper wire was coated with an ion-pair membrane matrix, resulting in a distribution of many electroactive sites on the surface. A metal oxide nanocomposite with different physical and

chemical properties, such as ZnO/CuO nanocomposite, was incorporated into the membrane composition to enhance the conductivity of the sensor surface due to its high conductivity, dielectric permittivity, mechanical and chemical stability, and



large surface area, which enhanced the PSD ions in the sample solution and the active sites distributed on the membrane surface<sup>36</sup>.

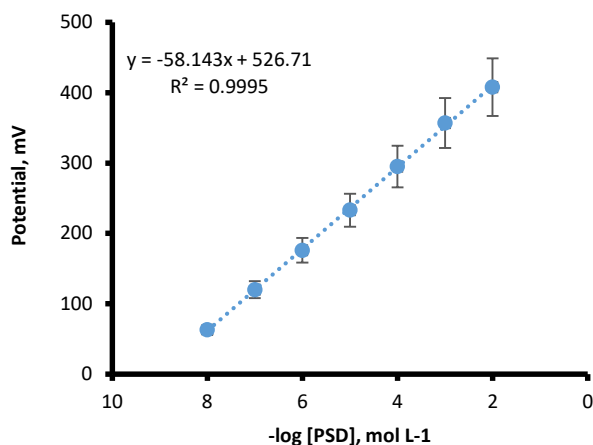


**Figure 6.** The calibration curve of the PSD-PT-ZnO/CuO nanocomposite using PSD concentration range of  $1.0 \times 10^{-8}$  -  $1.0 \times 10^{-2}$  mol L<sup>-1</sup>

#### Effect of Response Time and Soaking Time

The response time of the sensor PSD-PT-ZnO/CuO nanocomposite was constant 30 s, over the tested  $1.0 \times 10^{-3}$  mol L<sup>-1</sup> PSD solution. The reproducibility of the proposed sensor was investigated during their lifetime and the results showed high repeatability. The sensors have lifetimes of 80 days, and the slope of the sensor remained stable and repeatable throughout. By immersing the developed sensors for 1 to 6 hrs and overnight, the effect of immersion times on the potential activities of the sensors was investigated. It was found that the appropriate conditioning time for the prepared modified membrane was 3 hrs.

#### Effect of pH

Interference from hydrogen ions can have a significant effect on the potential reading of the membrane sensor. Therefore, it is important to determine the safe pH range in which hydrogen ions do not interfere with the potential reading of the sensor. The results showed that both PSD-PT-ZnO/CuO nanocomposite sensor concentrations are essentially pH-independent in the pH range of 3-6, and PSD can be accurately measured within this pH range using the proposed sensor Fig. 7. At lower pH values the increase in mV readings may be attributed to the interference of hydronium ion. While, at higher pH values the decrease in the mV readings may be

due to base precipitates in the test solution and consequently, the concentration of unprotonated species gradually increased<sup>10</sup>.

The obtained results may be understood as follows: at the pH levels below 3, as the number of hydrogen ions in the test solution increased, the sensor's potential also climbed somewhat due to forming a protonated ion pair resistant to the PSD ions. Nevertheless, at the pH levels above 6, the potential readings rapidly reduced because of a rise in the OH ions, causing competition between the PSD ions and the OH ions and, as a consequence, decreasing the interaction between the ion-pair sites on the sensor membrane and the ions of the drug being tested. As a result, the possible responses of the proposed sensor decreased<sup>45</sup>.

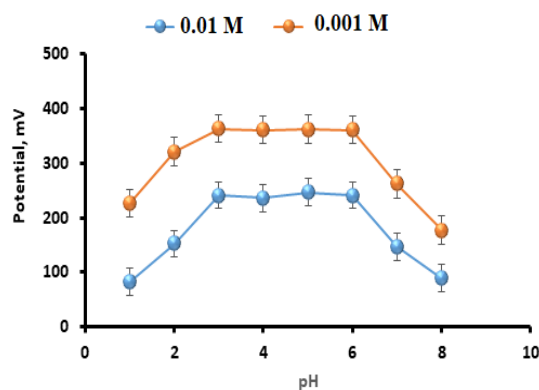


**Figure 7.** The effect of pH on the suggested PSD-PT-ZnO/CuO nanocomposite sensor using  $1.0 \times 10^{-3}$  mol L<sup>-1</sup> and  $1.0 \times 10^{-2}$  mol L<sup>-1</sup> PSD solutions

#### Effect of Foreign Substances

Separate and mixed solution methods were used to test the selectivity coefficient of the proposed sensor for identifying PSD in a mixture containing  $1.0 \times 10^{-3}$  mol L<sup>-1</sup> of PSD and interfering species. The proposed sensor showed excellent selectivity. The conductivity of the constructed sensor increased due to the large surface area and physicochemical properties of the metal oxide nanoparticles, which also improved the sensor's selectivity for the tested PSD ions. The results showed that carbohydrates and amino acids had no influence. In addition, the smaller in size, mobility and permeability of the inorganic cations compared to PSD<sup>+</sup> prevented these cations from interfering with the analysis of the drug. Therefore, using the PSD-PT-ZnO/CuO nanocomposite sensor to determine PSD<sup>+</sup>, high selectivity and good tolerance were achieved Table 3.

**Table 3. The selectivity coefficient ( $K^{Pot}_{PSD+}$ ) of the PSD-PT-ZnO/CuO nanocomposite sensor by the method of separate solution using  $1.0 \times 10^{-3} \text{ mol L}^{-1}$  PSD**

Interfering species	$K^{Pot}_{PSD+}$ of PSD-ZnO-CuO NPs sensor
Sodium ion	$4.3 \times 10^{-4}$
Silver ion	$5.2 \times 10^{-4}$
Calcium ion	$3.7 \times 10^{-5}$
Barium ion	$4.1 \times 10^{-5}$
Copper (II)ion	$2.6 \times 10^{-4}$
Ferric ion	$6.6 \times 10^{-4}$
Chloride ion	$1.9 \times 10^{-4}$
Sulphate ion	$3.9 \times 10^{-5}$
Phosphate ion	$2.2 \times 10^{-4}$
Fructose*	$1.1 \times 10^{-5}$
Glucose*	$7.4 \times 10^{-5}$
Sucrose*	$6.8 \times 10^{-5}$
Histidine*	$8.9 \times 10^{-5}$
Glycine *	$2.5 \times 10^{-5}$
Starch*	$4.6 \times 10^{-4}$

\*These compounds measured using mixed solution method

#### Quantitative Determination of PSD in Its Bulk Powder

The constructed PSD-PT-ZnO/CuO nanocomposite sensor was employed for determining PSD in its bulk powder and the percentage recovery was  $99.64 \pm 0.62$  for the proposed sensor Table 4. The high

sensitivity was due to the unique chemical and physical properties of the added nanoparticles of metal oxide, causing an excellent selectivity and sensitivity toward the examined drug because of the high dielectric constant of the nanocomposite of ZnO/CuO.

**Table 4. The results from quantifying PSD in bulk form using PSD-PT-ZnO/CuO nanocomposite sensor using PSD concentration range of  $1.0 \times 10^{-8}$  -  $1.0 \times 10^{-2} \text{ mol L}^{-1}$**

PSD-PT-ZnO-CuO nanocomposite sensor.			
	Taken -log [PSD]. $\text{mol L}^{-1}$	Found -log [PSD] $\text{mol L}^{-1}$	Recovery, %
Statistical analysis	8.0	8.02	100.25
	7.0	6.93	99.00
	6.0	5.97	99.50
	5.0	4.96	99.20
	4.0	4.02	100.50
	3.0	3.00	100.00
	2.0	1.98	99.00
%Mean±SD		99.64±0.62	
n		7	
Variance		0.38	
%SE		0.23	
%RSD		0.62	

#### Validation of the Proposed Potentiometric Method

According to “the standards of the International Council for Harmonization of Technical Requirements for Pharmaceuticals for Human Use (ICH)”<sup>48</sup>, the proposed potentiometric approach was validated. The PSD-PT-ZnO/CuO nanocomposite sensor displayed linear concentration ranges using the least square regression equation  $E_{mV} = (-58.143) \log [\text{PSD}] + 526.71$  with a correlation coefficient of 0.9995. After the slope of the suggested sensor was

lowered by 17.9 mV, the potential readings of the construction sensor were measured to establish the lower limit of detection (LOD). According to the obtained data, the recommended coated wire sensor had LODs of  $5.2 \times 10^{-9} \text{ mol L}^{-1}$ . The suggested sensor's accuracy was examined using the eight PSD concentrations, and a mean percentage recovery of  $99.60 \pm 0.3$  was determined. Additionally, the recommended potentiometric method's precision was verified using intra-day and inter-day assessments.



The percentage relative standard deviation (% RSD) was used to express the results. For intra-day and inter-day assessment, the proposed sensor displayed

0.49% and 1.11%, respectively. The fact that all findings are less than 2% suggests a very accurate approach Table 5.

**Table 5. The precision assay of the suggested method using PSD-PT -ZnO/CuO nanocomposite sensor using PSD concentration range of  $1.0 \times 10^{-8}$  -  $1.0 \times 10^{-2}$  mol L<sup>-1</sup>**

Statistical analysis	PSD-PT-ZnO/CuO nanocomposite coated copper wire sensors.					
	Intra-day assay			Inter-day assay		
	Taken -log [PSD]. mol.L <sup>-1</sup>	Found -log [PSD] mol L <sup>-1</sup>	Recovery, %	Taken -log [PSD]. mol L <sup>-1</sup>	Found -log [PSD] mol L <sup>-1</sup>	Recovery %
	8.0	7.96	99.50	8.0	7.94	99.25
	5.0	5.02	100.40	5.0	4.93	98.60
	3.0	2.98	99.33	3.0	3.03	101.00
	2.0	1.99	99.50	2.0	2.01	100.50
<b>%Mean±SD</b>		99.68±0.49			99.83±1.11	
<b>n</b>		4			4	
<b>Variance</b>		0.24			1.23	
<b>%SE</b>		0.25			0.20	
<b>%RSD</b>		0.49			1.11	

By utilizing phosphate buffer pH 5.5 to create a small variation in the pH values of the tested solutions, the robustness of the approach was investigated. The obtained percentage recovery was estimated and determined to be  $98.3 \pm 1.50$  for the suggested sensor (Table 2). The robustness of the recommended approach was further investigated using the EUTECH pH700 pH meter, another pH meter model. The outcome was shown as the mean percentage recovery for the indicated sensors, which was determined to be  $99.1 \pm 0.98$  (Table 2). There was no apparent distinction between the results and those produced using the approach provided, which verified a great agreement.

#### Determination of the PSD Quantity in Commercial Products

Three commercial products, syrup® (15 mg/5 mL), acetamol® tablet (30 mg/tablet), and Congestal® (60 mg/tablet) were used to determine the PSD content in their products. Regression equations were used to estimate recoveries as a percentage, with values for the test solutions ranging from  $1.0 \times 10^{-8}$  -  $1.0 \times 10^{-2}$  mol L<sup>-1</sup>. For the abovementioned sensor, the results were  $100.09 \pm 0.92$ ,  $99.79 \pm 0.98$ , and  $99.85 \pm 0.75$  for each product, respectively Table 6. The obtained results were compared with the previously reported spectrophotometric method<sup>23</sup> and statistically analyzed using Student's t-test and F-test<sup>49,50</sup>. The results showed that there were no significant differences between the two results.

**Table 6. The results from the determination of PSD in some pharmaceutical formulations using suggested PSD-PT -ZnO/CuO nanocomposite sensor using PSD concentration range of  $1.0 \times 10^{-8}$ - $1.0 \times 10^{-2}$  mol L<sup>-1</sup> in comparison with a spectrophotometric published approach<sup>23</sup>**

Samples	PSD-PT -ZnO/CuO nanocomposite sensor		
	Taken -log [PSD], mol L <sup>-1</sup>	Found-log [PSD] mol L <sup>-1</sup>	Recovery, %
Syrup	8.0	7.95	99.38
	7.0	7.03	100.43
	6.0	6.01	100.17
	5.0	4.98	99.60
	4.0	3.95	98.75
	3.0	3.04	101.33
	2.0	2.02	101.00
	<b>%Mean±SD</b>	100.09±0.92	
	<b>n</b>	7	
	<b>Variance</b>	0.85	
<b>%SE</b>	0.35		
<b>%RSD</b>	0.92		
Acetamol® tablet (30 mg/tablet)	8.0	8.02	100.25
	7.0	7.01	100.14
	6.0	6.05	100.83
	5.0	4.99	99.80
	4.0	3.92	98.00
	3.0	2.97	99.00
	2.0	2.01	100.50
	<b>*%Mean±SD</b>	99.79±0.98	
	<b>n</b>	7	
	<b>Variance</b>	0.96	
<b>%SE</b>	0.37		
<b>%RSD</b>	0.98		
Congestal® (60 mg/tablet)	8.0	8.06	100.75
	7.0	6.97	99.57
	6.0	6.01	100.17
	5.0	5.04	100.80
	4.0	3.96	99.00
	3.0	2.99	99.67
	2.0	1.98	99.00
	<b>*%Mean±SD</b>	99.85 ± 0.75	
	<b>n</b>	7	
	<b>Variance</b>	0.56	
<b>%SE</b>	0.28		
<b>%RSD</b>	0.75		
<b>Reported Method</b>	102.5±1.92		
<b>Mean±SD</b>			
<b>t-test</b>	2.03(2.23)*		
<b>F-test</b>	4.26 (5.05)*		

\* "The figures between parentheses are the theoretical values of " t-test" and "F-test" at P=0.05 <sup>49,50</sup>

## Conclusion

In the present approach, a potentiometric sensor based on ZnO/CuO nanocomposites was successfully constructed, characterized with easy modification and extreme sensitive. The sensor was fabricated by coating ZnO/CuO nanocomposites on a copper wire in the presence of PSD-PT (ion pair)

and *o*-NPOE as a plasticizer. The enormous surface-to-volume ratio of the proposed modified nanosensor provided tremendous sensitivity. The modified PSD-PT-ZnO/CuO nanocomposite sensor showed very high sensitivity and selectivity for the determination and quantification of PSD with a linear relationship

of  $1.0 \times 10^{-8}$ - $1.0 \times 10^{-2}$  mol L<sup>-1</sup> and a regression equation  $E_{mv} = (-58.143) \log [\text{PSD}] + 526.71$ . Statistical analysis was used to analyze the modified metal oxide nanocomposite sensor's outcomes in determining PSD. In addition, a metal oxide nanocomposite layer coated on the sensor surface improved the electrical conductivity of this sensor

### Acknowledgment

The authors would like to thank Department of Chemistry in the College of Science at Tikrit

### Authors' Declaration

- Conflicts of Interest: None.
- We hereby confirm that all the Figures and Tables in the manuscript are ours. Furthermore, any Figures and images, that are not ours, have been included with the necessary permission for

### Authors' Contribution Statement

F.M.A, S.T.A, and M.F. E approved all parameters and supervised the practical study of all potentiometric measurements. The experiments were

and the detection of the studied drug with high selectivity and sensitivity. Therefore, the development of sensors with coated wires and modified membrane using metal oxide nanocomposites could be successfully used to quantify PSD in commercial products.

University in Iraq for using their facilities and equipment.

- re-publication, which is attached to the manuscript.
- Ethical Clearance: The project was approved by the local ethical committee at Tikrit University

### References

1. Abdoon FM, Hasan HM, Salman SA, Ameen ST, Birhan M. Exploiting of green synthesized silver nanoparticles using Capparis spinosa L. Fruit for spectrophotometric determination of diphenhydramine HCl in pure forms and commercial products. *J Exp Nanosci.* 2023; 18(1): 2161525. <https://doi.org/10.1080/17458080.2022.2161525>
2. Alarfaj NA, El-Tohamy MF. New functionalized polymeric sensor based nio/mngo nanocomposite for potentiometric determination of doxorubicin hydrochloride in commercial injections and human plasma. *Polymers (Basel).* 2020; 12(12): 3066. <https://doi.org/10.3390/polym12123066>
3. Shetti NP, Malode SJ, Nayak DS, Bagihalli GB, Kalanur SS, Malladi RS, et al. Fabrication of ZnO nanoparticles modified sensor for electrochemical oxidation of methdilazine. *Appl Surf Sci.* 2019; 496: 143656. <https://doi.org/10.1016/j.apsusc.2019.143656>
4. Shin KY, Mirzaei A, Oum W, Yu DJ, Kang S, Kim EB, et al. Enhancement of selective NO<sub>2</sub> gas sensing via Xenon ion irradiation of ZnO nanoparticles. *Sens Actuators B Chem.* 2023; 374: 132808. <https://doi.org/10.1016/j.snb.2022.132808>
5. Saadi H, Benzarti Z, Sanguino P, Pina J, Abdelmoula N, de Melo JSS. Enhancing the electrical conductivity and the dielectric features of ZnO nanoparticles through Co doping effect for energy storage applications. *J Mater Sci.: Mater Electron.* 2023; 34(2): 116. <https://doi.org/10.1007/s10854-022-09470-5>
6. Dejam L, Kulesza S, Sabbaghzadeh J, Ghaderi A, Solaymani S, Țălu Ștefan, et al. ZnO, Cu-doped ZnO, Al-doped ZnO and Cu-Al doped ZnO thin films: Advanced micro-morphology, crystalline structures and optical properties. *Results Phys.* 2023; 44: 106209. <https://doi.org/10.1016/j.rinp.2023.106209>
7. Zarzuela R, Almoraima Gil ML, Carretero J, Carbú M, Cantoral JM, Mosquera MJ. Development of a novel engineered stone containing a CuO/SiO<sub>2</sub> nanocomposite matrix with biocidal properties. *Constr Build Mater.* 2021; 303: 124459. <https://doi.org/10.1016/j.conbuildmat.2021.124459>
8. Korgaonkar K, Pollet BG, Seetharamappa J, Kalanur SS. Ecofriendly Synthesis of Tenorite (CuO) Nanoparticles Composite with β-cyclodextrin as an Electrochemical Sensor for the Determination of the Anticancer Drug Phloretin. *J Electrochem Soc.* 2023; 170(6): 067505. <https://doi.org/10.1149/1945-7111/ace009>

9. Thangamani C, Ponnar M, Priyadharshini P, Monisha P, Gomathi SS, Pushpanathan K. Magnetic behavior of Ni-doped CuO nanoparticles synthesized by microwave irradiation method. *Surf. Rev. Lett.* 2019; 26(5): 1850184. <https://doi.org/10.1142/S0218625X18501846>
10. Wu Q, He L, Jiang ZW, Li Y, Cao ZM, Huang CZ, et al. CuO nanoparticles derived from metal-organic gel with excellent electrocatalytic and peroxidase-mimicking activities for glucose and cholesterol detection. *Biosens Bioelectron.* 2019; 145: 111704. <https://doi.org/10.1016/j.bios.2019.111704>
11. Mansournia M, Ghaderi L. CuO@ZnO core-shell nanocomposites: Novel hydrothermal synthesis and enhancement in photocatalytic property. *J Alloys Compd.* 2017; 691: 171-177. <https://doi.org/10.1016/j.jallcom.2016.08.267>
12. Rahman MM, Alam MM, Asiri AM, Chowdhury S, Alruwais RS. Sensitive detection of citric acid in real samples based on Nafion/ZnO–CuO nanocomposites modified glassy carbon electrode by electrochemical approach. *Mater Chem Phys.* 2023; 293: 126975. <https://doi.org/10.1016/j.matchemphys.2022.126975>
13. Mubeen K, Irshad A, Safeen A, Aziz U, Safeen K, Ghani T, et al. Band structure tuning of ZnO/CuO composites for enhanced photocatalytic activity. *J Saudi Chem Soc.* 2023; 27(3): 101639. <https://doi.org/10.1016/j.jscs.2023.101639>
14. Alwash A. The Green Synthesize of Zinc Oxide Catalyst Using Pomegranate Peels Extract for the Photocatalytic Degradation of Methylene Blue Dye. *Baghdad Sci J.* 2020;7(3): 787-794. <https://doi.org/10.21123/bsj.2020.17.3.0787>.
15. Del-Toro-Sánchez CL, Rodríguez-Félix F, Cinco-Moroyoqui FJ, Juárez J, Ruiz-Cruz S, Wong-Corral FJ, et al. Recovery of phytochemical from three safflower (*Carthamus tinctorius* L.) by-products: Antioxidant properties, protective effect of human erythrocytes and profile by UPLC-DAD-MS. *J Food Process Preserv.* 2021; 45(9): e15765. <https://doi.org/10.1111/jfpp.15765>
16. Pandey VC, Kumar A. *Leucaena leucocephala*: An underutilized plant for pulp and paper production. *Genet Resour Crop Evol.* 2013; 60(3): 1165-1171. <https://doi.org/10.1007/s10722-012-9945-0>
17. Vadapalani Nallasivam L, Gokhale JS. Rheological, techno-functional, and physicochemical characterization of *Prosopis cineraria* (Sangri) seed gum: A potential food and pharmaceutical excipient. *J Food Process Preserv.* 2022; 46(5): e16519. <https://doi.org/10.1111/jfpp.16519>
18. Juliantoni Y, Hajrin W, Subaidah WA. Nanoparticle Formula Optimization of Juwet Seeds Extract (*Syzygium cumini*) using Simplex Lattice Design Method. *J. biol. Tropis.* 2020; 20(3): 416-422. <https://doi.org/10.29303/jbt.v20i3.2124>
19. Chargui H, Ghazghazi H, Essghaier B, Fradj MK Ben, Feki M, Charfi I, et al. Investigation on the Chemical Composition of Phenolic, Fatty Acid Profiles (GC-FID) and Biological Activities from *Leucaena leucocephala* (Lam de wit) Seed Oil and Leaves Extracts: Effect of Geographical Location and Maturation Stage. *Chem. Afr.* 2023; 6(2): 819–826. <https://doi.org/10.1007/s42250-022-00533-y>
20. Alemán-Ramirez JL, Okoye PU, Torres-Arellano S, Mejía-Lopez M, Sebastian PJ. A review on bioenergetic applications of *Leucaena leucocephala*. *Ind Crops Prod.* 2022; 182: 114847. <https://doi.org/10.1016/j.indcrop.2022.114847>
21. Głowacka K, Wiela-Hojeńska A. Pseudoephedrine—benefits and risks. *Int J Mol Sci.* 2022; 22(10): 5146. <https://doi.org/10.3390/ijms22105146>
22. Cartwright AC. *The British Pharmacopoeia, 1864 to 2014: Medicines, International Standards and the State. The British Pharmacopoeia, 1864 to 2014: Medicines, International Standards and the State*, Routledge, London, UK, 2016.
23. Pourbasheer E, Fathi Majd S, Azari Z, Ansari S, Ganjali MR. Magnetic solid-phase extraction and spectrophotometric determination of pseudoephedrine in real samples. *J Chin Chem Soc.* 2022; 69(3): 532-539. <https://doi.org/10.1002/jccs.202100542>
24. Ali MS, Elsaman T. Development and Validation of the UV Spectrophotometric Method for Simultaneous Determination of Paracetamol and Pseudoephedrine in Bulk and Combined Tablet Dosage Form. *Pharm Chem J.* 2021; 54(12): 1306-1310. <https://doi.org/10.1007/s11094-021-02360-w>
25. Reid IOA. Experimental Design Optimized Chromatographic Determination of Pseudoephedrine and Fexofenadine in Bulk and Tablets. *Pharm Chem J.* 2023; 56(10): 1426-1432. <https://doi.org/10.1007/s11094-023-02808-1>
26. Orman E, Assumang A, Oppong-Kyekyeku J, Onilimor PJ, Peparah PK, Adu JK, et al. Chromatographic method development for the simultaneous assay of pseudoephedrine hydrochloride and chlorphenamine maleate in oral dosage formulations. *Sci Afr.* 2022; 15: e01109. <https://doi.org/10.1016/j.sciaf.2022.e01109>
27. Lee S, Shim WS, Yoo H, Choi S, Yoon J, Lee KY, et al. A pharmacokinetic study of ephedrine and pseudoephedrine after oral administration of ojeok-san by validated LC-MS/MS method in human plasma. *Molecules.* 2021; 26(22): 6991. <https://doi.org/10.3390/molecules26226991>

28. Liu YM, Sheu SJ. Determination of ephedrine and pseudoephedrine in Chinese herbal preparations by capillary electrophoresis. *J Chromatogr A*. 1993; 637(2): 219-223. [https://doi.org/10.1016/0021-9673\(93\)83218-h](https://doi.org/10.1016/0021-9673(93)83218-h)
29. Ali MS, Elsaman T. Development and Validation of the UV Spectrophotometric Method for Simultaneous Determination of Paracetamol and Pseudoephedrine in Bulk and Combined Tablet Dosage Form. *Pharm Chem J*. 2021; 54(12): 107820. <https://doi.org/10.1016/j.microc.2022.107820>
30. Moustafa AA, Hegazy MA, Mohamed D, Ali O. Functionalized Fe<sub>3</sub>O<sub>4</sub> Magnetic Nanoparticle Potentiometric Detection Strategy versus Classical Potentiometric Strategy for Determination of Chlorpheniramine Maleate and Pseudoephedrine HCl. *J Anal Methods Chem*. 2019; 2019: 6947042. <https://doi.org/10.1155/2019/6947042>
31. Banga I, Paul A, Poudyal DC, Muthukumar S, Prasad S. Recent Advances in Gas Detection Methodologies with a Special Focus on Environmental Sensing and Health Monitoring Applications— A Critical Review. *ACS Sens*. 2023; 8(9): 3307–3319. <https://doi.org/10.1021/acssensors.3c00959>
32. Umapathi R, Ghoreishian SM, Sonwal S, Rani GM, Huh YS. Portable electrochemical sensing methodologies for on-site detection of pesticide residues in fruits and vegetables. *Coord. Chem. Rev*. 2022;453:214305. <https://doi.org/10.1016/j.ccr.2021.214305>
33. Adam H, Gopinath SC, Arshad MM, Adam T, Hashim U, Sauli Z, et al. Integration of microfluidic channel on electrochemical-based nanobiosensors for multiplex and multiplex analyses: An overview. *J Taiwan Inst Chem Eng*. 2023; 146: 104814. <https://doi.org/10.1016/j.jtice.2023.104814>
34. Gupta R, Raza N, Bhardwaj SK, Vikrant K, Kim KH, Bhardwaj N. Advances in nanomaterial-based electrochemical biosensors for the detection of microbial toxins, pathogenic bacteria in food matrices. *J Hazard Mater*. 2021; 401: 123379. <https://doi.org/10.1016/j.jhazmat.2020.123379>
35. Kushwaha CS, Abbas NS, Shukla SK. Chemically functionalized CuO/Sodium alginate grafted polyaniline for nonenzymatic potentiometric detection of chlorpyrifos. *Int J Biol Macromol*. 2022; 217: 902-909. <https://doi.org/10.1016/j.ijbiomac.2022.07.113>
36. Xu J, Huang Y, Zhu S, Abbas N, Jing X, Zhang L. A review of the green synthesis of ZnO nanoparticles using plant extracts and their prospects for application in antibacterial textiles. *J Eng Fibers Fabr*. 2021; 16: 15589250211046242. <https://doi.org/10.1177/15589250211046242>
37. Sadiq H, Sher F, Sehar S, Lima EC, Zhang S, Iqbal HM, et al. Green synthesis of ZnO nanoparticles from *Syzygium Cumini* leaves extract with robust photocatalysis applications. *J Mol Liq*. 2021; 335: 116567. <https://doi.org/10.1016/j.molliq.2021.116567>
38. Tabrizi Hafez Moghaddas SM, Elahi B, Javanbakht V. Biosynthesis of pure zinc oxide nanoparticles using Quince seed mucilage for photocatalytic dye degradation. *J Alloys Compd*. 2020; 821: 153519. <https://doi.org/10.1016/j.jallcom.2019.153519>
39. Yulizar Y, Bakri R, Apriandanu DOB, Hidayat T. ZnO/CuO nanocomposite prepared in one-pot green synthesis using seed bark extract of *Theobroma cacao*. *Nano-Structures and Nano-Objects*. 2018; 16: 300-305. <https://doi.org/10.1016/j.nanoso.2018.09.003>
40. Khit SA, Kareem ET, Shaheed IM. Eco-Friendly Synthesized of CuO Nanoparticles Using *Anchusa strigosa* L. Flowers and Study its Adsorption Activity. *Baghdad Sci J*. 2023; 20(4): 1322. <https://doi.org/10.21123/bsj.2023.7444>
41. Mohammadi-Aloucheh R, Habibi-Yangjeh A, Bayrami A, Latifi-Navid S, Asadi A. Green synthesis of ZnO and ZnO/CuO nanocomposites in *Mentha longifolia* leaf extract: characterization and their application as anti-bacterial agents. *J Mater Sci.: Mater Electron*. 2018; 29(16): 13596-13605. <https://doi.org/10.1007/s10854-018-9487-0>
42. Egorov V V., Zdrachek EA, Nazarov VA. Improved separate solution method for determination of low selectivity coefficients. *Anal Chem*. 2014; 86(8): 3693-3696. <https://doi.org/10.1021/ac500439m>
43. Aseel T, Abdul jabbar, Saadiyah A. Dahir, Waleed M. Abood. Furfural Removal from Simulated Wastewater Using ZnO Nanoparticles / H<sub>2</sub>O<sub>2</sub> in Solar Photocatalysis Reactor. *J Phys Conf Ser*. 2021; 1818: 012048. <https://doi.org/10.1088/1742-6596/1818/1/012048>
44. Siddheswaran R, Jeyanthi CE, Thangaraju K, Mangalaraja RV. Columnar structure growth of Mn-doped ZnO (MZO) thin films by radio frequency co-sputtering and studies on films properties. *Mater Technol*. 2022; 37(2): 79-85. <https://doi.org/10.1080/10667857.2020.1814053>
45. Okubo S, Ozeki Y, Yamada T, Saito K, Ishihara N, Yanagida Y, et al. Facile Fabrication of All-solid-state Ion-selective Electrodes by Laminating and Drop-casting for Multi-sensing. *Electrochem*. 2022; 90(7): 077001. <https://doi.org/10.5796/electrochemistry.22-00020>
46. Wahba ME., Ayman A, Zeid AM., Yasser ES., Draz ME. Portable and green solid contact potentiometric sensor for the rapid and direct assay of clozapine in post-mortem rat liver and dosage forms: An analytical approach to forensic and pharmaceutical

- samples. *Microchem J.* 2023; 186: 108364. <https://doi.org/10.1016/j.microc.2022.108364>
47. Akl ZF.. Rapid electrochemical sensor for uranium (VI) assessment in aqueous media. *RSC Adv.* 2022; 12(31): 20147-20155. <https://doi.org/10.1039/D2RA02619H>
48. European Medicines Agency. ICH guidelines Q2(R2) on validation of analytical procedures. ICH Harmonised Guideline. 2022; 2(0). <https://www.ema.europa.eu/en/ich-q2r2-validation-analytical-procedures-scientific-guideline>
49. Dhahir S A. Sunlight photocatalytic degradation of propanil in aqueous solution and determination of degraded products with UV-and HPLC. *Asian J Chem.* 2012; 24(12): 5490–5492.
50. Abdoon FM, Khaleel AI, El-Tohamy MF. Utility of electrochemical sensors for direct determination of nicotinamide (B3): Comparative studies using modified carbon nanotubes and modified  $\beta$ -cyclodextrin sensors. *Sens Lett.* 2015; 13(6): 462-470. <https://doi.org/10.1166/sl.2015.3498>

## متحسس ZnO/CuO النانوي الوظيفي الحيوي للتقدير الجهدى لهيدروكلوريد السيودايفيدرين في المنتجات النقية والتجارية

فدعم متعب عبدون<sup>1</sup>، سرحان علي سلمان<sup>1</sup>، حسن محمد حسن<sup>2</sup>، سهام توفيق أمين<sup>3</sup>، مها فاروق النهامي<sup>4</sup>

<sup>1</sup>قسم الكيمياء، كلية العلوم، جامعة تكريت، تكريت، العراق.

<sup>2</sup>كلية الصيدلة، جامعة تكريت، تكريت، العراق.

<sup>3</sup>كلية الصحة والتكنولوجيا الطبية، جامعة أروك، بغداد، العراق.

<sup>4</sup>قسم الكيمياء، كلية العلوم، جامعة الملك سعود، الرياض، المملكة العربية السعودية.

### الخلاصة

لقد ولدت الإمكانيات الوظيفية الفائقة لأكاسيد الزنك (ZnO) والنحاس (CuO) النانوية اهتمامًا كبيرًا باستخدام أكاسيد المعادن مثل المركبات النانوية المميزة والنشطة كهربائيًا في الدراسات المتعلقة بالقياسات الجهدية والمتحسسات. تم تحضير هذه الأكاسيد النانوية من مستخلص بذور شجرة اللبوسينا (*Leucaena leucocephala*) كطريقة صديقة للبيئة. إذ تم اقتراح تطوير متحسس غشائي من أسلاك النحاس المطلية بمركب نانوي ZnO/CuO كطريقة جديدة للتقدير الجهدى لهيدروكلوريد السيودايفيدرين (PSD) في أشكاله النقية وجرعاتها الصيدلانية. بوجود كلوريد البولي فينيل (PVC) كبوليمر ذو وزن جزيئي عالي و"أورثو- نيتروفينيل أوكثيل إيثر (o-NPOE) كوسيط مذيّب، تم دمج PSD مع حمض الفوسفونوجستنيك (PTA) لإنتاج هيدروكلوريد السيودايفيدرين- فوسفونوجستات (PSD-PT) كأساس للتحسس. أظهر المتحسس المحور حساسية وانتقائية عالية جدًا لتقدير وقياس PSD بعلاقة خطية تبلغ  $1.0 \times 10^{-2}$  مول لتر<sup>-1</sup>. وأظهرت معادلة الخط المستقيم (معادلة الإنحدار)  $EmV = (-58.143) \log [PSD] + 526.71$ . وباستخدام المتحسس المقترح، يمكن تقدير هيدروكلوريد السيودايفيدرين بشكل فعال في أشكاله النقية والمنتجات والتجارية.

**الكلمات المفتاحية:** هيدروكلوريد السيودايفيدرين، مركب أكسيد الزنك/النحاس النانوي، متحسس بوليمري، شجرة اللبوسينا *Lucaena leucocephala*، الكيمياء الخضراء.